

# Fractional-Order MOS Capacitor: Experimental Results and Monte Carlo Analysis

Lucas Almir dos Santos Fernandes<sup>1</sup>, Marco Isaias Alayo<sup>1</sup> and Joao Antonio Martino<sup>1</sup>

<sup>1</sup>Polytechnic School, University of Sao Paulo, Sao Paulo, Brazil  
e-mail: lucasalmir@usp.br

**Abstract**—In this work, an experimental implementation of a Fractional-order MOS capacitor using a fractal tree structure in discrete circuits was carried out in order to validate the theoretical results obtained of the simulations. In addition, a Monte Carlo analysis was performed to determine the sensitivity of the electrical circuit to the variation of some parameters. In these analyzes were observed that for a tolerance of 20% in the device values and for  $2\sigma$  above and below the median values (for both, width, and initial frequency value of fractal zone) it is noticed a deviation of 18% and -14%, respectively, which is a reasonable deviation for a group that contains more than 90% of the samples.

**Index Terms**— Fractal zone, fractional-order MOS capacitor, fabrication mismatch, Monte Carlo simulation, Fractal Tree implementation.

## I. INTRODUCTION

Fractional-order capacitors are components in which the impedance can be described by fractional-order derivatives or integrals. The impedance of a fractional-order capacitor can be written as  $Z(s) = \frac{1}{Cs^\eta}$  in the Laplace Domain, where  $\eta$  can assume any real value between 0 and 1 [1]. It is important to detail that for a conventional capacitor,  $\eta$  would be constant and equal to 1.

Some authors have already studied the impact of replacing conventional capacitors with fractional-order capacitors in known circuits [2, 3, 4]. In Wien Bridge's case, for example, if the integer-order capacitor could be replaced by a  $\alpha$ -order capacitor with the same value  $C$ , the oscillation frequency of the system becomes  $\omega = \frac{1}{(RC)^\frac{1}{\eta}}$ , showing that it is possible to

obtain very high oscillation frequencies when  $0 < \eta < 1$  [2]. For example, if  $RC = 10^{-6}$ s and  $\eta = \frac{1}{2}$ ,  $\omega$  would increase from  $10^6$  rad/s to  $10^{12}$ rad/s.

There is a wide variety of works demonstrating that some fractal geometric pattern circuits follow the behaviour of a fractional component on a specific frequency region called *Fractal Zone* and it depends on the kind of pattern structure and on the number of iterations [5, 6, 7].

An important fractal structure is known as Fractal Tree, which was studied by several authors [8, 9, 10] and implemented experimentally using a microelectronic fabrication process based on MOS technology.

Figure 1 shows the cross section of a conventional MOS capacitor which would be used as basic component for the implementation of a Fractal Tree structure. At the same figure, an equivalent electrical circuit schematic of the conventional MOS capacitor is also showed.

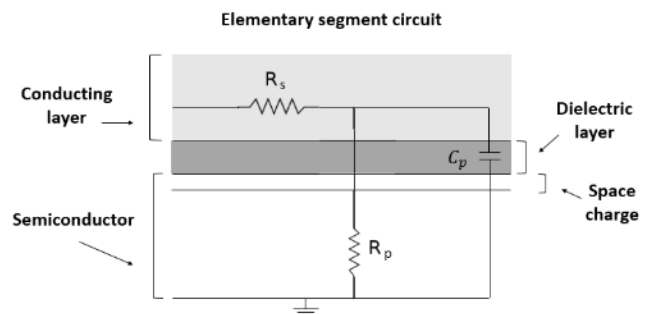


Fig. 1. Cross-section of a conventional MOS capacitor and its equivalent circuit schematic diagram—the circuit of an elementary segment of the Fractal Tree [9]

The process to obtain the Fractal Tree structure is characterized as follows:

1. In the iteration 0 the Fractal Tree is started with a segment of Length  $L$  (Figure 2.a).
2. The segment is divided into 3 equal parts of length  $L/3$  (so, forming 2 junctions) (Figure 2.b). In the first junction it is added a segment of Length  $L/3$  forming a  $\Theta$  angle (Note that now we have 5 segments of  $1/3$  of the previous length).
3. The next iterations will be characterized by the repetition of step 2 for each segment individually.

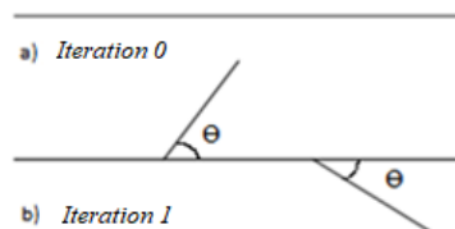


Fig. 2. Iterations 0 (a) and 1 (b) of a Fractal Tree.

It is easy to see that  $L_i = \frac{L}{3^i}$  and  $N_i = 5^i$ , where  $i$  is the number of iterations,  $L_i$  the length of each basic element and  $N_i$  the number of elements at iteration  $i$ . As obtaining the Fractal Tree is an iterative process, it is necessary to make some distinctions. For example, there is a difference between the "elementary series resistance" (associated with the most elementary segment of the structure - which was "divided"  $i$  times) and the "total series resistance" (associated with an "unsplit" segment). Therefore, the "total series resistance"  $R_s$ , "total capacitance"  $C_p$ , and "total parallel resistance"  $R_p$  are related, respectively with the "elementary series resistance"  $R_{se}$ , "elementary capacitance"  $C_{pe}$ , and "elementary parallel resistance"  $R_{pe}$  by:

- $R_s = \frac{R_{se}}{3^i}$
- $C_p = \frac{C_{pe}}{3^i}$
- $R_p = 3^i R_{pe}$

There are many definitions of the dimension of a fractal structure. One of the definitions is that the dimension of a fractal structure can be interpreted as a measure of its complexity and is defined as  $D_f = \log(\alpha)/\log(\beta)$ , where  $\alpha$  is the number of elements that increase with each iteration, and  $\beta$  is the reduction factor. Particularly, for the Fractal Tree the dimension is  $D_f = \log(5)/\log(3) = 1.46$ .

It can be shown that under appropriate conditions, the impedance equation can be written as  $Z(\omega/(\alpha\beta)) = \beta Z(\omega)$ , where a possible solution for this equation can be written as  $Z(\omega) = \frac{k}{(j\omega)^\eta}$ . Doing some manipulations is possible to obtain the following expression  $\eta = \frac{\log(\beta)}{\log(\alpha)+\log(\beta)}$ , which for the Fractal Tree results in  $\eta = 0.406$ . As  $\eta$  is related to the argument by the expression  $\theta = -\frac{\pi}{2}\eta$ , then the theoretical argument ( $\theta$ ) for a Fractal Tree structure is -36 degrees [9].

## II. IMPEDANCE: SIMULATIONS AND PROPERTIES

In order to obtain impedance  $Z$  of the Fractal Tree, a simple way is to treat the different iterations of the circuit as Linear Two-Port Networks and derive recursive equations between them. As the Linear Two-Port Network of the same iteration have the same parameters, the impedance is easily calculated by a bottom-up approach. The relationships among voltages and currents of a Linear Two-Port Network are showed in equation 1.

$$\begin{cases} \mathbf{I}_{j1} = \mathbf{a}_j \mathbf{I}_{j2} + \mathbf{b}_j \mathbf{V}_{j2} \\ \mathbf{V}_{j1} = \mathbf{c}_j \mathbf{I}_{j2} + \mathbf{d}_j \mathbf{V}_{j2} \end{cases} \quad (1)$$

Where  $j$  denotes the iteration, 1 if it is an input measurement and 2 if it is an output measurement.

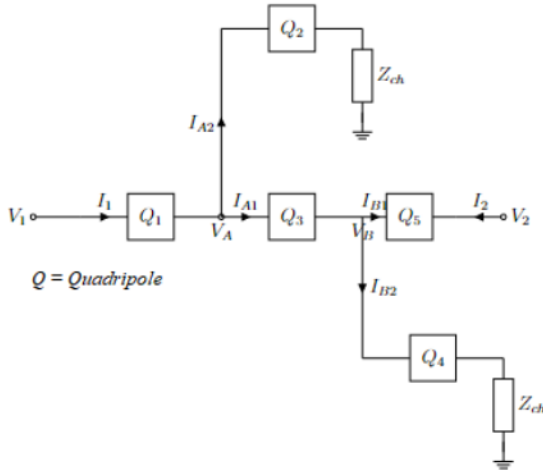


Fig.3. Scheme for calculating the parameters of the next iteration. The term  $Z_{ch}$  refers to “infinite impedance”

Using the scheme of figure 3 to solve the equation, it is possible to find the following recursive relations among the parameters:

$$a_{j+1} = F_j(a_j, b_j)a_j + c_j(F_j(a_j, b_j)\frac{b_j}{d_j} + G_j(a_j, b_j)) \quad (2a)$$

$$b_{j+1} = F_j(a_j, b_j)b_j + d_j(F_j(a_j, b_j)\frac{b_j}{d_j} + G_j(a_j, b_j)) \quad (2b)$$

$$c_{j+1} = F_j(c_j, d_j)a_j + c_j(F_j(c_j, d_j)\frac{b_j}{d_j} + G_j(c_j, d_j)) \quad (2c)$$

$$d_{j+1} = F_j(c_j, d_j)b_j + d_j(F_j(c_j, d_j)\frac{b_j}{d_j} + G_j(c_j, d_j)) \quad (2d)$$

Where:

$$F_j(\mathbf{x}, \mathbf{y}) = \mathbf{x} \mathbf{a}_j - \mathbf{c}_j(\mathbf{y} - \mathbf{x} \frac{b_j}{d_j}) \quad (3a)$$

$$G_j(\mathbf{x}, \mathbf{y}) = -\mathbf{x} \mathbf{b}_j + \mathbf{d}_j(\mathbf{y} - \mathbf{x} \frac{b_j}{d_j}) \quad (3b)$$

With the equations 2 and 3, a fractal tree of any iteration level can be easily simulated. For this work, all simulations were performed in Python programming language [11].

The typical curve of the argument of a Fractal Tree can be seen in Figure 4.

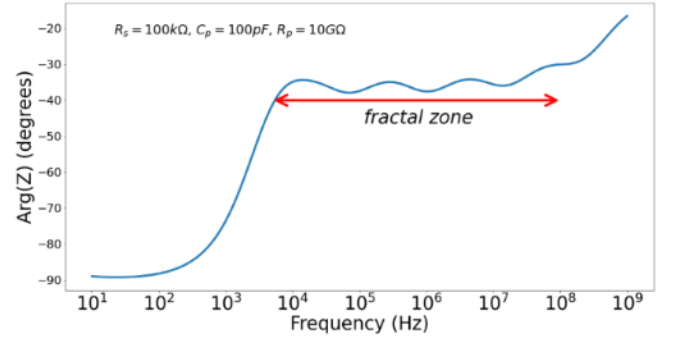


Fig.4. Impedance argument curve of a Fractal Tree using  $R_s = 100\text{k}\Omega$ ,  $C_p = 100\text{pF}$  and  $R_p = 10\text{G}\Omega$  and 5 iterations.

Simulating for different values of  $R_p$  it was observed that the value of this component has influence only at low frequencies (below  $10^{-2}$  Hz) and not in the Fractal Zone (Figure 5). As in this work we are just interested in the Fractal Zone and so, the influence of  $R_p$  will be neglected and the value of  $R_p$  will be considered infinite for the simulations.

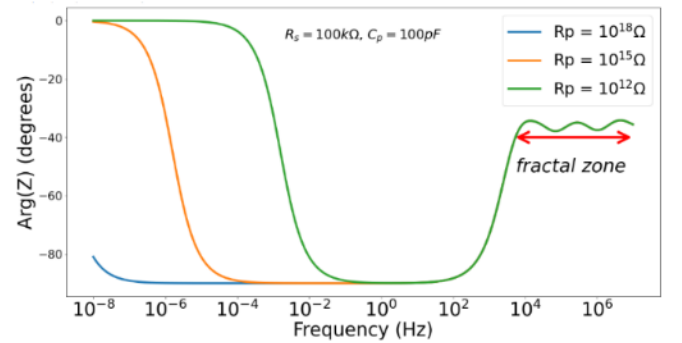


Fig.5. Impedance argument curves using  $R_s = 100\text{k}\Omega$ ,  $C_p = 100\text{pF}$ , 5 iterations, and different  $R_p$  values

In figure 6 can be observed that the argument curve for the medium and high frequencies will always be the same as long as the  $R_s \times C_p$  product is constant.

By varying the  $R_s \times C_p$  product, the argument curve is shifted linearly on a frequency logarithmic scale, being inversely proportional to the product  $R_s \times C_p$  (Figure 7). So,

given a certain frequency  $f_0$  obtained due to a specific pair  $(R_{s0}, C_{p0})$ , if the pair is changed to  $(R_{s1}, C_{p1})$ , we can obtain the new frequency  $f_1$  using the following equation (4).

$$f_1 = f_0 \frac{R_{s0}C_{p0}}{R_{s1}C_{p1}} \quad (4)$$

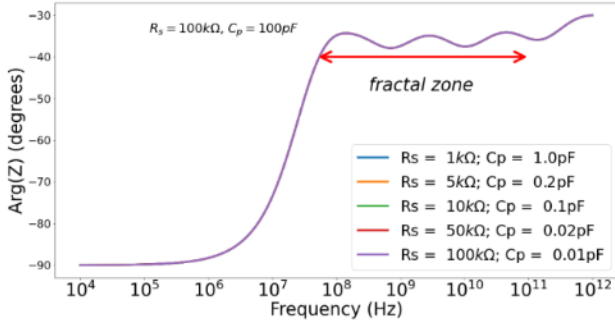


Fig.6. Impedance argument for different  $C_p$  and  $R_s$ , using infinite  $R_p$  and 5 iterations. In this figure the product  $R_s C_p$  is kept constant.

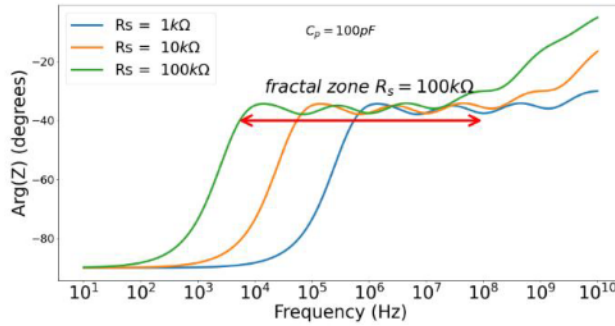


Fig.7. Impedance argument for  $C_p = 100\text{pF}$ , infinite  $R_p$ , 5 iterations and different  $R_s$  values.

Another important aspect is that the fractal zone (frequency width) depends on the number of iterations, the higher number of iterations, the larger the fractal zone, as can be seen in Figure 8.

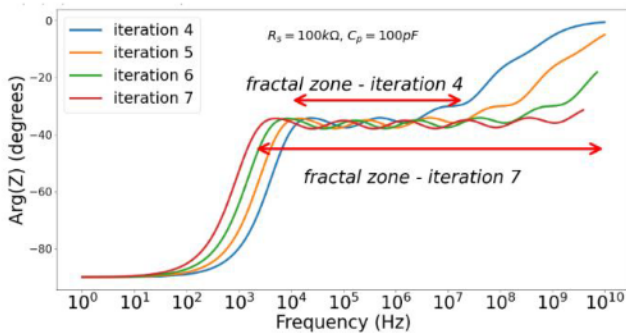


Fig.8. Different iterations using  $R_s = 100\text{k}\Omega$ ,  $C_p = 100\text{pF}$  and infinite  $R_p$ .

In this work, it will be defined the width of the Fractal Zone as the region where the argument lies between two constant values. In this work we will use the values  $-32$  and  $-40$  degrees as the limits to the Fractal Zone, therefore, a variation of 4 degrees around the theoretical value of  $-36$  degrees (figure 9).

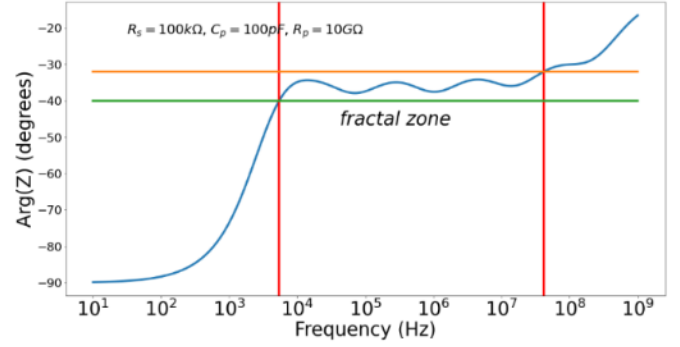


Fig.9. Fractal Zone highlighted for  $R_s = 100\text{k}\Omega$ ,  $C_p = 100\text{pF}$  and infinite  $R_p$ . In this example the initial frequency is  $5432\text{Hz}$  and the frequency width is  $4.18 \times 10^7\text{Hz}$ .

### III. EXPERIMENTAL RESULTS

To confirm the theoretical description and the simulations presented, experiments with discrete circuits were performed.

Three experiments were carried out, for iterations 1, 2 and 3. For each of the configurations,  $R_{se} = 82\Omega$  and  $C_{pe} = 92\text{pF}$  were used as elementary components.

The main equipment used for this experimental characterization were:

- An Agilent 33500B Series Function Generator
- A Keysight DSOX2002A Oscilloscope
- LabVIEW 2014 software to make getting results easier and faster

The measurement circuit is composed by the function generator – configured to generate a peak-to-peak 20V sine wave over a range of frequencies from 1kHz to 1MHz, by a resistor of value  $R$  and by the fractal circuit of impedance  $Z$ .

The probes of the oscilloscope were positioned such as showed in figure 10 and using as reference the “ground” of the electrical circuit.

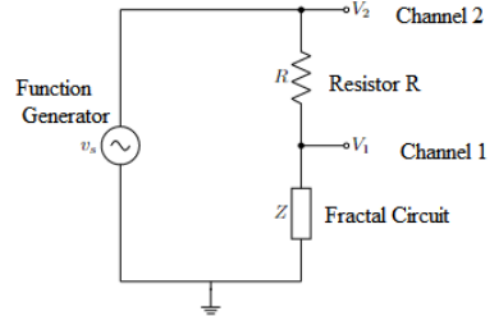


Fig.10. Measurement Circuit.

From the circuit shown in Figure 10, it is easy to conclude that

$$Z = \frac{-RV_1}{V_1 - V_2} \quad (5)$$

The equations of  $\text{mod}(Z)$  and  $\text{arg}(Z)$  are then

$$\text{mod}(Z) = \frac{-|R||V_1|}{|V_1 - V_2|} \quad (6a)$$

$$\text{arg}(Z) = 180^\circ + \text{arg}(V_1) - \text{arg}(V_1 - V_2) \quad (6b)$$

The values of  $|V_1|$ ,  $|V_2|$ ,  $\text{arg}(V_1)$  and  $\text{arg}(V_1 - V_2)$  are obtained directly through the functionalities of the

oscilloscope, thus, for a given frequency value, just have to use equations (6a) and (6b), thus building the curves of  $\text{mod}(Z)$  and  $\text{arg}(Z)$ .

In figure 11 and 12 we can observe the  $\text{arg}(Z)$  and  $\text{mod}(Z)$  as a function of the frequency for both, simulated and experimental results for 1, 2 and 3 iterations.

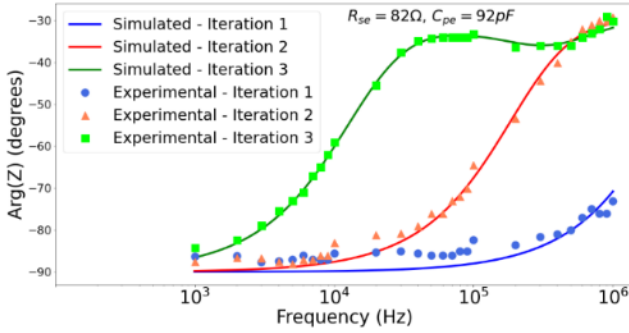


Fig. 11. Comparing  $\text{arg}(Z)$  from simulations and experiments for different iterations – all with elementary components  $R_{se} = 82\text{k}\Omega$ ,  $C_{pe} = 92\text{pF}$  and infinite  $R_p$ .

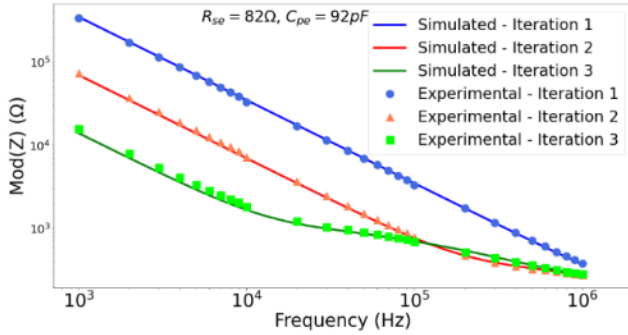


Fig. 12. Comparing  $\text{mod}(Z)$  from simulations and experiments for different iterations – all with elementary components  $R_{se} = 82\text{k}\Omega$ ,  $C_{pe} = 92\text{pF}$  and infinite  $R_p$ .

Such as it can be seen in the figures, there is a good agreement of the argument and modulus of the Fractal Tree of the simulated and experimental results demonstrating that it was used an appropriated theoretical approach.

#### IV. MONTE CARLO ANALYSIS

In microelectronics, it is very common to have a substantial variation on devices fabricated in different runs [12]. Thinking in the implementation of a Fractal Tree using components fabricated on Microelectronics technology and knowing the significant variations on the values of these devices using this technology, it is interesting to visualize how the properties of the Fractal Tree are influenced by the variations of these parameters. To proceed with the evaluations, the Monte Carlo Method was used in this work, and the samples will be taken on the parameters  $R_s$  and  $C_p$  and it will be evaluated the distributions of the initial frequency and the width of the Fractal Zone. For the parameters to be sampled, it will be assumed that the distribution of its perturbation is a Gaussian with a standard deviation (written as  $\sigma$ ) such that there is a tolerance of 20% up to  $3\sigma$ . It is well known that in a Gaussian distribution,  $1\sigma$  corresponds to 68.27%,  $2\sigma$  to 95.45% and  $3\sigma$  to 99.71% of the deviations around the mean. As reference values will be used  $R_s=100\text{k}\Omega$ ,  $C_p=100\text{pF}$ , infinite  $R_p$  and 3 iterations – it is important to make it clear that the perturbations will be made on the elementary parameters, which are

$R_{se}=3.7\text{k}\Omega$  and  $C_{pe}=3.7\text{pF}$ . To analyse the distribution of the initial frequency and the width of the fractal zone, 50000 samples of simultaneous variation of  $R_s$  and  $C_p$  will be used. The initial frequency and the width of the Fractal Zone are 14.6 kHz and 502 kHz for the reference values of  $R_s$  e  $C_p$ , respectively.

To evaluate the distribution more empirically, it will be used the median, and the percentiles since that the simulated curves did not show a gaussian pattern. So, whenever a specific percentile is mentioned, this value would be identical to its counterpart in the Gaussian curve. For example, when about a percentile is  $2\sigma$  above the median, it means that this value corresponds to  $95.45/2\% = 47.72\%$  above the median in the distribution.

The Monte Carlo distribution for the width of the fractal zone is shown in figure 13.

The median and the percentiles of the Monte Carlo analysis for the width of the fractal zone are shown in table 1.

It is possible to see in table I that the deviations, although significant, do not change the order of magnitude of the width of the fractal zone. For  $2\sigma$  above and below it is noticed a deviation of 18% and -14%, respectively, which is a reasonable deviation for a group that contains more than 90% of the samples.

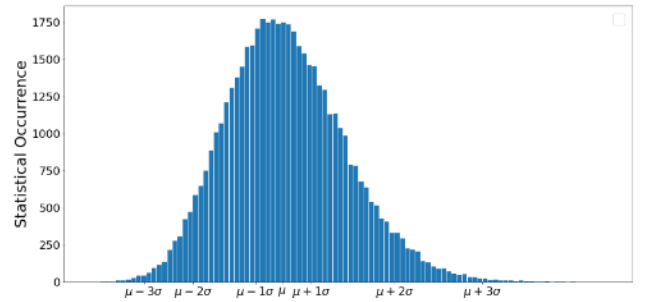


Fig. 13. Histogram of the width of the Fractal Zone.

Table I. Fractal zone width distribution statistics

3σ below the median	391 kHz	-22%
2σ below the median	431 kHz	-14%
1σ below the median	481 kHz	-4%
Median	503 kHz	
1σ above the median	526 kHz	5%
2σ above the median	593 kHz	18%
3σ above the median	664 kHz	32%

The Monte Carlo distribution for the initial frequency is shown in figure 14.

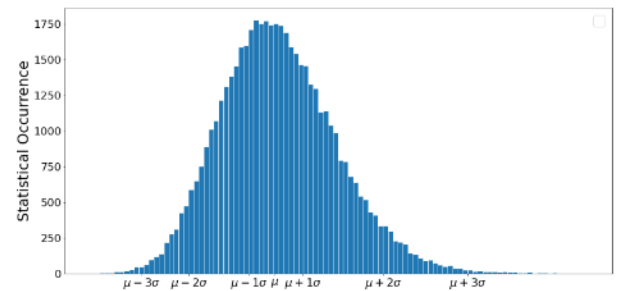


Fig. 14. Histogram of the Initial Frequency of the Fractal Zone

The median and the percentiles of the Monte Carlo analysis for the initial frequency are shown in table 2.

Table II. Initial frequency distribution statistics

3 $\sigma$ below the median	11.3 kHz	-23%
2 $\sigma$ below the median	12.5 kHz	-14%
1 $\sigma$ below the median	14 kHz	-4%
Median	14.6 kHz	
1 $\sigma$ above the median	15.3 kHz	5%
2 $\sigma$ above the median	17.2 kHz	18%
3 $\sigma$ above the median	19.3 kHz	32%

For the initial frequency, the deviations associated with the percentiles are practically the same when compared to the width of the fractal zone, which is expected, since that both are inversely proportional to the product  $R_s \times C_p$ .

## V. CONCLUSION

In this work, important properties of the Fractional-order MOS Capacitor with a fractal tree structure were analyzed demonstrating the validity of the theoretical basis with experiments carried out in discrete components. Comparing the experiments with the simulations, a good agreement was obtained with the argument and modulus of the Fractal Tree. In addition, the Monte Carlo technique was used to analyze the sensitivity of the properties of width and initial frequency of the Fractal Zone, and the results indicated that for a simultaneous variation of the values of  $R_s$  and  $C_p$  with a tolerance of 20%, an asymmetrical variation is observed for width and initial frequency of fractal zone. For 2 $\sigma$  above and below the median values (for both, width and initial frequency value of fractal zone) it is noticed a deviation of 18% and -14%, respectively, which is a reasonable deviation for a group that contains more than 90% of the samples. However, if greater precision is desired of the Fractal Zone characteristics, more restrictive tolerance values must be used for the resistance and capacitance parameters.

## ACKNOWLEDGMENTS

The authors would like to thank CNPq and CAPES for the financial support.

## REFERENCES

- [1] A. S. Elwakil, "Fractional-order circuits and systems: An emerging interdisciplinary research area," in *IEEE Circuits and Systems Magazine*, vol. 10, no. 4, pp.40-50, Fourthquarter 2010, doi: 10.1109/MCAS.2010.938637.
- [2] W. Ahmad, R. El-Khazali and A. S. Elwakil, "Fractional-order Wien-bridge oscillator," in *Electronics Letters*, vol. 37, no. 18, pp. 1110-1112, 30 Aug. 2001, doi:10.1049/el:20010756.
- [3] Maundy, B., Elwakil, A. Gift, S. On a multivibrator that employs a fractional capacitor. *Analog Integer Circuit Signal -Processing* 62, 99 (2010). <https://doi.org/10.1007/s10470-009-9329-3>.
- [4] A. G. Radwan, A. M. Soliman, and A. S. Elwakil, "First order filters generalized to the fractional domain," *J. Circuits Syst. Comput.*, vol. 17, pp. 55–66, 2008.
- [5] Carlson, G. E., Halijak, C. A. (1964). Approximation of fractional capacitors (1/s) 1/n by regular newton process. *IEEE Transactions on Circuit Theory CT*, 11(2), 210–213.
- [6] Clerc JP, Tremblay AMS, Albinet G, Mitescu CD. ac response of fractal networks. *J Phys Lett* 1984;45:L913–924
- [7] Liu SH. Fractal model for the ac response of rough interface. *Phys Rev Lett* 1985;55:529–32.
- [8] Cisse Haba T, Ablart G, Camps T. The frequency response of a fractal photolithographic structure. *IEEE, Trans Dielectrics. Electric Insul* 1997;4(3).
- [9] C. Haba, G. Ablart, T. Camps, and F. Olivie, "Influence of the electrical parameters on the input impedance of a fractal structure realized on silicon," *Chaos, Solitons Fractals*, vol. 24, pp. 479–490, 2005.
- [10] Haba, T, Cisse & Loum, Georges L. & Ablart, G., 2007. "An analytical expression for the input impedance of a fractal tree obtained by a micro-electronical process and experimental measurements of its non-integral dimension," *Chaos, Solitons & Fractals*, Elsevier, vol. 33(2), pages 364-373
- [11] Van Rossum G, Drake FL. *Python 3 Reference Manual*. Scotts Valley, CA: CreateSpace; 2009
- [12] B. Sutbas, E. Ozbay and A. Atalar, "Accurate and Process-Tolerant Resistive Load," in *IEEE Transactions on Microwave Theory and Techniques*, vol. 68, no. 7, pp. 2495-2500, July 2020, doi: 10.1109/TMTT.2020.2986207.